Bimolecular Fluorescence Complementation of Alpha-synuclein Demonstrates its Oligomerization with Dopaminergic Phenotype in Mice

EBioMedicine 29 (2018) 13–22

Contents lists available at ScienceDirect

EBioMedicine

journal homepage: www.ebiomedicine.com

Research Paper

Bimolecular Fluorescence Complementation of Alpha-synuclein Demonstrates its Oligomerization with Dopaminergic Phenotype in Mice

Waijiao Cai [a,b], Danielle Feng [b], Michael A. Schwarzschild [b], Pamela J. McLean [c], Xiqun Chen [b,a,*]

[a] Shanghai Huashan Hospital, Fudan University, Shanghai, China
[b] MassGeneral Institute for Neurodegenerative Disease, Department of Neurology, Massachusetts General Hospital, Harvard Medical School, Boston, USA
[c] Mayo Clinic, Jacksonville, FL, USA

ARTICLE INFO

Article history:
Received 15 December 2017
Received in revised form 22 January 2018
Accepted 25 January 2018
Available online 31 January 2018

Keywords:
Parkinson's disease
Alpha-synuclein
Mouse model
Oligomers
Neuroinflammation

ABSTRACT

Alpha-synuclein (αSyn) is encoded by the first causal gene identified in Parkinson's disease (PD) and is the main component of Lewy bodies, a pathological hallmark of PD. aSyn-based animal models have contributed to our understanding of PD pathophysiology and to the development of therapeutics. Overexpression of human wildtype αSyn by viral vectors in rodents recapitulates the loss of dopaminergic neurons from the substantia nigra, another defining pathological feature of the disease. The development of a rat model exhibiting bimolecular fluorescence complementation (BiFC) of αSyn by recombinant adeno-associated virus facilitates detection of the toxic αSyn oligomers species. We report here neurochemical, neuropathological and behavioral characterization of BiFC of αSyn in mice. Overexpression and oligomerization of αSyn through BiFC is detected by conjugated fluorescence. Reduced striatal dopamine and loss of nigral dopaminergic neurons are accompanied neuroinflammation and abnormal motor activities. Our mouse model may provide a valuable tool to study the role of αSyn in PD and to explore therapeutic approaches.

1. Introduction

Parkinson's disease (PD) is the second most common neurodegenerative disorder manifested by slowness in movement, muscular rigidity, rest tremor, postural and gait impairment, and non-motor features. Available dopaminergic treatments offer symptomatic relief. However, there is currently no therapy to slow, halt, or reverse its progressive course. Pathologically, loss of dopaminergic neurons in the substantia nigra (SN) and presence of Lewy bodies and Lewy neurites in the residual neurons are hallmarks of PD (Braak and Del Tredici, 2009). The main component of Lewy bodies is insoluble aggregates of alpha-synuclein (αSyn), a ubiquitously expressed neuronal protein. While native state and functions of αSyn are not completely understood, increasing evidence suggests that soluble oligomeric αSyn is the most toxic species (Dehay et al., 2015; Kingwell, 2017). Although the etiology of PD is unclear, neuroinflammation appears to be an important contributor to its pathogenesis (Hirsch et al., 2005; Hirsch and Hunot, 2009; Hirsch and Vyas, 2012).

αSyn is encoded by *SNCA*, the first gene identified to cause PD (Spillantini et al., 1997). Multiple copies and point mutations of *SNCA* lead to the early onset of familial PD, and αSyn also contributes the basis of genetic risk of developing sporadic PD (Kalinderi et al., 2016). Given the central role of αSyn in PD genetics and pathogenesis, various animal models overexpressing either wildtype (WT) or mutant forms of αSyn have been developed to model the disease and to develop therapies. Among these models, viral vector-mediated overexpression of αSyn offers several advantages in recapitulating dopaminergic pathology of PD (Koprich et al., 2017). Using targeted overexpression of human WT αSyn in the SN by recombinant adeno-associated virus (AAV), we and others demonstrated loss of nigral dopaminergic neurons and neuroinflammatory responses in both rats and mice (Harms et al., 2013; McFarland et al., 2009; Theodore et al., 2008). The development of a bimolecular fluorescence complementation (BiFC) assay in rats facilitates direct detection of overexpression of αSyn fused to the N- and C- terminus half of venusYFP and formation of αSyn oligomers. The rat model shows striatal gliosis, neuritic dystrophy and loss of nigral dopaminergic neurons (Dimant et al., 2013).

Here we report systematical characterization of this BiFC system in mice including neuropathological, neurochemical, synucleinopathic, neuroinflammatory and behavioral changes. Time courses and dose responses were explored, with comparison to the original non-BiFC system. Since mice are the most commonly used animal species in PD research and most genetic probes are readily available in mice, our mouse model may provide a valuable tool to explore new therapeutic approaches for PD.

* Corresponding author at: 114, 16th Street Room 3003, Charlestown, MA 02129, USA.
E-mail address: xchen17@mgh.harvard.edu (X. Chen).

https://doi.org/10.1016/j.ebiom.2018.01.035

2. Materials and Methods

2.1. Mice

Adult C57BL/6J mice (4–5 months old, male and female, weighing 25–30 g) from the Jackson laboratory were used for all experiments. Animals were randomly assigned to different groups. Animals were maintained in home cages at constant temperature with a 12-h light/dark cycle and free access to food and water. All experiments were performed in accordance with a protocol approved by the Massachusetts General Hospital Animal Care and Use Committee and in compliance with the National Institute of Health guidelines for the use of experimental animals.

2.2. Viral Vectors

BiFC vectors: (1) pAAV-CBA-Venus1-human αSyn -WPRE (V1S) by inserting the human WT *SNCA* fused with N-terminus half of venusYFP into the *Eco*RV and *Nhe*I sites of pAAV-CBA-WPRE vector; (2) pAAV-CBA- human αSyn -venus2-WPRE (SV2) by inserting the human WT *SNCA* fused with C-terminus half of venusYFP into the EcoRV and NheI sites of pAAV-CBA-WPRE vector; (3) pAAV-CBA-venusYFP-WPRE (venus) by inserting the venusYFP into the *Xho*I and NheI sites of pAAV-CBA-WPRE vector (Dimant et al., 2013).

Non-BiFC vectors: (1) pAAV-CBA- human αSyn -WPRE (αSyn) by inserting the human WT *SNCA* into the XhoI and NheI sites of pAAV-CBA-WPRE vector (St Martin et al., 2007; Theodore et al., 2008); (2) pAAV-CBA-WPRE empty vector (vector).

All vectors were packaged and purified in AAV serotype 8 by the Mayo Clinic Viral Vector laboratory.

2.3. Stereotaxic Virus Injections

Mice were anesthetized by intraperitoneal injection of Avertin and were placed in a stereotaxic frame. A total volume of 2 μl of virus was infused unilaterally at a rate of 0.1 ul/min into the left SN at coordinates at AP 0.09, ML 0.12, and DV -0.43 cm with lambda as a point of reference. At the end of the injection, the needle remained in place for 5 min before gradual removal.

The final injection titers (genome copies (gc)/ml) were: 5.1×10^{12} for V1SSV2 (mixing V1S at 4.7×10^{12} and SV2 at 5.4×10^{12} with equal volumes); 0.6×10^{12} and 4.4×10^{12} for venus. 3.9×10^{12} and 7.8×10^{12} for αSyn; 7.7×10^{12} for vector.

Authors who performed viral injections were blind to vector group information. Sample sizes were determined by power calculation to provide 80% power to detect 20–30% biologically meaningful changes in primary outcome measure (nigral dopaminergic neuron counts) based on our published estimates of mean ± SEM among WT (Chen et al., 2013) and one-way ANOVA with Tukey post-hoc test at $p < 0.05$.

2.4. Behavioral Testing

Locomotor activity was assessed using the open field test as described (Chen et al., 2017; Graham and Sidhu, 2010). Mice were placed in the activity chamber (11 × 11 in. with clear 8-in. high walls) and monitored by an infrared video tracking system for 10 min (Ethovision XT 9.0, Noldus Information Technology, The Netherlands). Tests were conducted in the first hour of the dark cycle on two consecutive days. Averages of the distance traveled, active time duration and velocity from the two sessions were calculated.

Amphetamine-induced (5 mg/kg *i.p.*) rotational behavior was assessed in an automated rotometry system (San Diego Instruments) for 60 min as described previously (Chen et al., 2017).

2.5. Immunostaining and Quantitative Analysis

Animals were sacrificed, and their brains were dissected, post-fixed in 4% paraformaldehyde overnight, cryoprotected in 30% sucrose and sectioned coronally as previously described (Chen et al., 2017). Sections were processed accordingly and incubated with primary antibodies. Primary antibodies were: mouse monoclonal antibody against αSyn (Thermo Fisher Scientific Cat# AHB0261, RRID:AB_2536241, at 1:500), mouse monoclonal antibody against pSer129-αSyn (BioLegend Cat# 825701, RRID:AB_2564891, at 1:500), mouse monoclonal antibody against astrocytes marker glial fibrillary acidic protein (GFAP, Sigma-Aldrich Cat# G3893, RRID:AB_477010, at 1:2500), rabbit monoclonal antibody against microglia marker ionized calcium-binding adapter molecule 1 (iba-1, Abcam Cat# ab178846, RRID:AB_2636859, at 1:2000), and rabbit polyclonal antibody against dopaminergic neuron marker tyrosine hydroxylase (TH, Enzo Life Sciences Cat# BML-SA497-0100, RRID:AB_2052772, at 1:1000). For peroxidase staining, sections were incubated with appropriate secondary antibodies and the staining was developed by incubating with 3,3′-Diaminobenzidine (DAB). For fluorescent TH staining, sections were incubated with goat anti-rabbit lgG-Alexafluor 546 Alexa (Thermo Fisher Scientific Cat# A-11010, RRID:AB_2534077, at 1:1000). Sections were covered by ProLong™ Gold Antifade Mountant with 4′,6-diamidino-2-phenylindole (DAPI) nuclear staining after serial washes.

For analysis of GFAP staining and YFP fluorescence intensity, images were captured under an Olympus BX50 microscope (Olympus Optical Co., Tokyo, Japan) with a DP 70 digital camera system using the same camera gain, exposure time and pixel setting for all sections. Integrated optical density (IOD) of GFAP staining in images taken under ×40 objective was analyzed by Image J. Two midbrain sections containing the central and anterior SN per mouse were analyzed. YFP fluorescence average intensity above background in the ipsilateral SN was analyzed by ImageJ using images taken under ×10 objective.

Morphology of iba1-positive cells in the SN pars compacta (SNpc) was analyzed and classified according to the published method by Sanchez-Guajardo et al. (2010). Based on their morphological characteristics, iba1-positive cells were classified as resting (type A, visible thin cytoplasm with long and thin processes), activated (type B, dense and enlarged cell body with thick, short processes), and phagocytic (type C, pseudo-amoeboid shape, big, dark cell body merging with processes) microglia. Cells were classified and counted cell by cell using stereological method at 40× magnification (Olympus BX51 microscope and Olympus CAST stereology software) as previously described (Dimant et al., 2013; West et al., 1991). Two midbrain sections containing the central and anterior SN per mouse were analyzed. Percentage of each cell type was calculated.

2.6. Stereological Analysis of Nigral Dopaminergic Neurons

For dopaminergic neuron counts, a complete set of serial SN sections at 30 μm from each animal was stained for TH and counterstained for Nissl substance (Chen et al., 2013, 2017). Sections were coded and the number of TH-positive cells was counted by unbiased stereology based on the optical fractionator principle using Olympus BX51 microscope and Olympus CAST stereology software, as previously described (Dimant et al., 2013; West et al., 1991).

2.7. Proteinase K Digestion

Proteinase K (PK) digestion was performed as previously reported (Dimant et al., 2013). Briefly, brain sections were mounted on the slides, and dry sections were rehydrated in TBS buffer containing 0.05% tween-20 (PH7.4). Sections were then treated with 50 μg/ml PK at 55 °C for 120 min.

2.8. Sequential Tissue Extraction and Immunoblot Analysis of Human αSyn

Animals were sacrificed and ventral midbrain and striatum were dissected. Protein sequential extraction was conducted as previously reported with some modifications (Harms et al., 2013). Briefly, tissues were homogenized in RIPA buffer containing 1% Triton X-100 and protease inhibitor then centrifuged. Supernatants were designated as "Triton X-100 soluble" fractions. Pellets were resuspended in TBS buffer containing 10% SDS and protease inhibitor and centrifuged. The supernatants were designated as "SDS soluble" fractions. Fractions were then subjected to NuPAGE SDS-PAGE gel (Thermo Fisher Cat#NP0322), and Western blot analysis was performed using anti-human αSyn antibody (Thermo Fisher Scientific Cat# AHB0261, RRID:AB_2536241, at 1:1000). Pan-actin (Thermo Fisher Scientific Cat# MS-1295, RRID:AB_63314) was probed as loading control. After incubation with secondary antibodies, signal was detected using enhanced chemiluminescence.

2.9. Measurement of Dopamine Content

Animals were sacrificed and striatum were dissected. Dopamine (DA) content was determined by standard high-performance liquid chromatography (HPLC) with electrochemical detection, as previously described (Chen et al., 2013; Xiao et al., 2006).

2.10. Statistical Analysis

Tissue process and outcome assessments were conduct in blind manner wherever possible. All values are expressed as mean ± SEM. The difference between groups was analyzed by Student's *t*-test or ANOVA followed by Tukey post hoc test when an overall significance was demonstrated. $p < 0.05$ is considered statistically significant.

3. Results

3.1. AAV8-mediated Human WT αSyn Overexpression in the SN, and αSyn Oligomerization Detected by BiFC in Mice

Increasing evidence supports that pathologic αSyn oligomers are strongly correlated to neurodegeneration in PD (Bengoa-Vergniory et al., 2017; Kalia et al., 2013). BiFC is a powerful and widely used tool to study protein-protein interactions in vitro and in vivo (Paulmurugan et al., 2004; Tetzlaff et al., 2008). As illustrated in Fig. 1a, Venus is fragmented into N and C termini, then fused with human WT αSyn to form non-fluorescent fusion proteins V1S and SV2, respectively (Dimant et al., 2013). When αSyn forms oligomers, the fused complementary N- and C-terminal halves of venusYFP combine, reconstituting a full, fluorescent complex. Therefore, venusYFP fluorescence can serve as an indicator for αSyn oligomerization.

The V1S SV2 mixture as well as venus control were injected into the SN. At 4 weeks post-injection, venusYFP fluorescence (green) was observed in the SN both in venus-injected and in V1SSV2-injected mice (Fig. 1b). Colocalization with TH immunofluorescence revealed successful transduction and reconstitution of venusYFP upon αSyn oligomerization in nigral dopaminergic neurons. No fluorescence was observed in the non-injected contralateral side. All sections were counterstained with 4′, 6-diamidino-2-phenylindole (DAPI, blue) to visualize nuclei.

To further confirm AAV human αSyn transduction in the SN, we performed immunoperoxidase staining using a human specific αSyn antibody at 4 weeks after V1SSV2 injection. Positively stained cells were observed in the entire SN on the ipsilateral side (Fig. 1c). No specific staining was detected on the contralateral side as expected (Fig. 1c). Fluorescent staining also showed robust human αSyn transduction on the injection side in V1SSV2-injected mice. Colabeling for TH revealed transduction and oligomerization of αSyn in dopaminergic neurons in the SN (Fig. 1d). To assess whether αSyn detected by conjugated venusYFP is soluble oligomers, SN sections were treated by proteinase K. VenusYFP fluorescence was diminished after the treatment. This result suggests soluble nature of αSyn oligomerization at 4 weeks post-AAV injection (Fig. 1e).

3.2. Nigral Overexpression of Human WT αSyn Induces Synucleinopathy in the SN and Striatum

To determine whether targeting human WT αSyn overexpression to the SN leads to pathological characteristics, coronal sections containing SN and striatum were examined by fluorescence microscopy. Intense venusYFP fluorescence in the ipsilateral SN was observed under low magnification in animals 8 weeks after injection with venus or V1SSV2 (Fig. 2a). VenusYFP fluorescence in the ipsilateral striatum was also visible. Higher magnification revealed fluorescence in both cell bodies and projections. In the striatum fluorescent fibers but no cell profiles were observed, confirming specific, anterograde transduction of venus or V1SSV2 and αSyn oligomerization along the nigrostriatal dopaminergic projections (Fig. 2a). No fluorescence was observed in the contralateral sides of SN and striatum. Despite their similar fluorescence intensity and localization, venus and V1SSV2 groups showed different fluorescence patterns. While smooth and more evenly distributed in cell bodies and fibers in venus-injected mice, a beaded and punctate venusYFP fluorescence pattern was observed in the SN and the striatum of V1SSV2-injected animals (Fig. 2a). The abnormal venusYFP fluorescent structures were colabeled with TH, indicating dopaminergic αSyn pathology (Fig. 2a).

To assess again whether αSyn aggregates detected by venusYFP is soluble at a later time point, SN sections from mice sacrificed at 12 weeks following V1SSV2 injection were treated with proteinase K. Following proteinase K treatment, venusYFP fluorescence was mostly absent. This result suggests that majority of αSyn multimers assembled by this time were still soluble oligomers. However, few remaining visible venusYFP puncta after proteinase K treatment may indicate formation of insoluble αSyn aggregates (Fig. 2b).

To further investigate synuclein pathologies in V1SSV2 mice, midbrain sections from V1SSV2 mice 12 weeks post-injection were immunostained for pSer129-αSyn, a phosphorylated αSyn modification at serine 129 that correlates to αSyn aggregation and progressive neurodegeneration of PD (Anderson et al., 2006). pSer129-αSyn positive signal was observed in the ipsilateral SN reticulata (SNr) as well as SNpc while no specific staining was found on the contralateral side (Fig. 2d). High magnification showed round, condensed staining with some beading similar to the reconstituted venusYFP fluorescence pattern. To probe the dominant species of αSyn in our model, we employed Western blot using a human αSyn antibody. Sequential extractions of the ventral midbrain and the striatum dissected from non-BiFC αSyn-injected mice at 8 weeks post-transduction were analyzed. Multiple high-molecular-weight bands of αSyn were detected in both the midbrain and the striatum ipsilateral to the injection side, indicating oligomerization and formation of toxic, high-molecular-weight αSyn species from virus transduction (Fig. 2e). Visible bands on the contralateral side, which has been observed in a previous study using same αSyn 211 antibody (Harms et al., 2013) might be explained by cross-reaction of the antibody with endogenous mouse αSyn that was not detectable by immunohistochemistry (Fig. 1c) but became detectable by Western blot using sequential tissue extraction.

3.3. Human WT αSyn Overexpression Induces Astrogliosis and Microgliosis

Chronic neuroinflammation is associated with dopaminergic neurodegeneration in PD (Hirsch and Hunot, 2009; More et al., 2013; Perry and Holmes, 2014). Abnormal αSyn accumulation activates immune cells, including brain resident astrocytes and microglia (Dimant et al., 2013; Harms et al., 2013). To assess whether targeted BiFC αSyn overexpression in the SN induces concomitant inflammatory responses,

midbrain coronal sections from mice at 12 weeks post-injection were analyzed (Fig. 3). Animals injected with V1SSV2 or venus were immunostained for the astrocyte marker GFAP and microglia marker iba-1. While venus injection did not change GFAP, there was significantly more GFAP immunoreactivity on the ipsilateral side compared to the contralateral side in V1SSV2 group as confirmed by IOD assessment

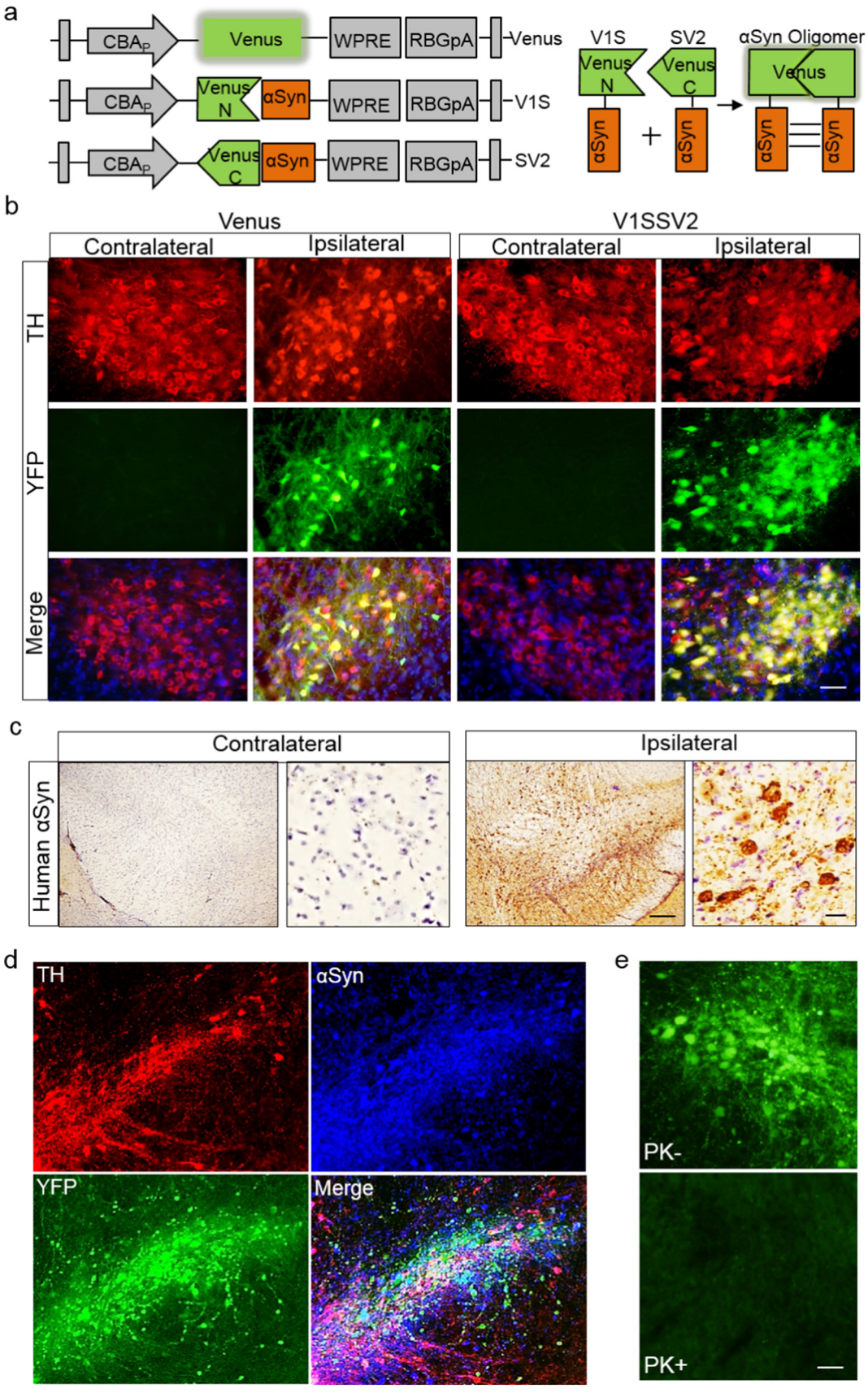

(Fig. 3a and b). Astrocytes on the ipsilateral side in V1SSV2-injected mice displayed enlarged bodies and ramifications, indicating activation of these cells (Fig. 3a) (Braak et al., 2007).

Morphology-based classification (Sanchez-Guajardo et al., 2010) was employed to analyze microglia activation after virus transduction. Microglia undergo significant morphological changes from resting, thin cell bodies with numerous branched extensions to activate, enlarged cell bodies with fewer short and thick branches to pseudo-amoeboid shaped phagocytic state. We identified and counted the three subtypes of iba-1 stained cells. Microglia in venus-injected mice were mostly resting cells. V1SSV2 transduction resulted in a significant increase in activated microglia and their further transformation to phagocytic microglia. No phagocytic microglia were observed in venus-injected mice (Fig. 3c and d). These data support that human WT αSyn overexpression triggered inflammatory responses in the SN.

3.4. Human WT αSyn Overexpression Leads to Abnormal Motor Behavior

To access motor activities in our mouse AAV αSyn models, open field and rotational behavior tests were performed. Open field was tested 14 weeks after non-BiFC αSyn and vector virus injection and before sacrifice. Interestingly, αSyn mice tended to be more active. They showed increased distance covered, movement duration time and velocity compared to vector controls as shown in Fig. 4a, b, c and in representative movement tracks at 7 min of a total 10 min session in Fig. 4d. Since our models are unilateral, we assessed amphetamine-induced rotational behavior in animals injected with V1SSV2 and venus control virus at 11 weeks post-injection (Chen et al., 2013, 2017). Amphetamine induces release and inhibits reuptake of DA in the striatum leading to predominantly ipsilateral turning behavior in animals with unilateral nigrastriatal lesions (Brooks and Dunnett, 2009; Iancu et al., 2005). While venus-injected mice did not tend to turn towards either side, there was an unexpected trend towards more contralateral turn and less ipsilateral turns in V1SSV2 mice, and V1SSV2 animals exhibited a significant increase in contralateral turns vs ipsilateral turns following amphetamine stimulation (Fig. 4e).

3.5. Reduced Striatal DA Content Induced by Human WT αSyn Overexpression in the SN

To characterize dopaminergic phenotypes in our mouse AAV αSyn models, we assessed striatal DA content using HPLC. Since YFP can potentially cause toxicity, we injected mice with higher (4.4×10^{12} gc/ml, venus-H) and lower (0.6×10^{12} gc/ml) doses of venusYFP and compared venusYFP at these two titers with non-BiFC empty vector at 7.7×10^{12} gc/ml. At 12 weeks post-injection, there was 3%, 8%, and 25% decrease in striatal DA content relative to the contralateral side in vector, venus and venus-H group, respectively (Fig. 5a). The decrease in venus-H group is statistically significant compared with the contralateral side, indicating toxicity of venusYFP at 4.4×10^{12} gc/ml, not AAV8 vector itself, even at a higher titer.

To exclude this venusYFP toxicity, we measured venusYFP fluorescence intensity in V1SSV2 (5.08×10^{12} gc/ml) and venus control 4 weeks post-injection, when transduction was robust as shown in Fig. 1. While venusYFP fluorescence intensity in V1SSV2 and venus group showed no difference, venus-H group exhibited 2.4-fold higher fluorescence intensity compared to V1SSV2 (Fig. 5b). Based on these results, we selected venus group with matching fluorescence intensity as control for V1SSV2.

To assess whether there was a time effect of αSyn transduction on striatal DA, we analyzed DA levels at 4 and 12 weeks after venus and V1SSV2 injection (Fig. 5c and d). A 10%, non-significant decrease at 4 weeks and a significant 38% reduction at 12 weeks in striatal DA on the injection side were revealed in V1SSV2 group. No significant striatal DA reduction was detected at either time point in venus group. These results suggest progressive nigrostriatal lesion induced by αSyn over a 12-week timeframe.

We also evaluated striatal DA levels in mice injected non-BiFC αSyn at 3.9×10^{12} gc/ml and a higher titer at 7.8×10^{12} gc/ml (αSyn-H) and vector at 7.7×10^{12} gc/ml. αSyn at these two titers led to 24% and 50% reductions in striatal DA, respectively, at 12 weeks post-injection, significant changes compared to vector-injected control animals. BiFC V1SSV2 (at 5.04×10^{12} gc/ml) on the other hand led to a 33% decrease in striatal DA, also a significant difference from control venus (at 0.6×10^{12} gc/ml, with matching venus fluorescence) group (Fig. 5e). In addition, diminished density of striatal TH staining in V1SSV2-injected mice on the injection side was indicated (Fig. 5f). These results suggest dose- and time- dependent DA reduction induced by AAV αSyn.

3.6. Loss of Nigral Dopaminergic Neurons Induced by Human WT αSyn Overexpression

To assess whether human WT αSyn overexpression led to loss of dopaminergic neurons, serial midbrain sections were immunostained for TH and the number of TH-positive cells were counted by an unbiased stereological method. V1SSV2-injected mice had 3460 ± 201 TH-positive neurons on the side ipsilateral to the injection, statistically different from 4897 ± 238 on the contralateral non-injection side at 12 weeks following virus injection, and statistically different from the lesion side of venus-injected mice (5090 ± 452), which showed no change in TH-positive cells on the injection side compared with contralateral non-injection side (Fig. 6 a and b). Nissl counterstaining and stereological counting of TH-negative neurons in the SNpc revealed no difference between contralateral and ipsilateral sides in V1SSV2 group. Nor was there difference in number of TH-negative neurons on the ipsilateral side between venus and V1SSV2 groups (Fig. 6b). Total counts of TH-positive and TH-negative cells, which reflect total number of neurons in the SNpc were significantly lower on the ipsilateral side in V1SSV2-injected mice as compared to venus-injected mice (4640 ± 225 vs 6223 ± 501, $p < 0.05$). The total counts on the ipsilateral side were also lower in the SNpc in V1SSV2-injected mice when comparing to the contralateral side of the same group (4640 ± 225 vs 6056 ± 258, $p < 0.05$). These findings support αSyn-mediated toxicity in the SNpc at 12 weeks was dopaminergic neuron-specific.

To characterize the time course of dopaminergic cell loss, we assessed an earlier time point, 4 weeks post-transduction and a later time point, 22 weeks post-injection along with the 12 weeks time point. Consistent with striatal DA changes, there were 8%, 29% and 33% losses of dopaminergic neuron counts at 4, 12 and 22 weeks, respectively (Fig. 6c). These results suggest progressive dopaminergic neurodegeneration induced by αSyn injection between 4 weeks and 12 weeks and a relative plateau state after to up to 22 weeks.

4. Discussion

Tremendous effort has been made to generate αSyn-based genetic animal models of PD since the identification of αSyn mutations in familial PD. Transgenic and AAV-mediated animal models overexpressing

Fig. 1. AAV8-mediated human WT αSyn expression in the SN and αSyn oligomerization detected by BiFC in mice at 4 weeks post-AAV injection. (a) Schematic structures of venus and αSyn-BiFCs (V1S and SV2). Upper right illustrates reconstitution of venusYFP fluorescence by αsyn-αsyn interactions. (b) TH immunofluorescence and venusYFP fluorescence in the SN. Tissue sections were counterstained with DAPI (blue). Scale bar: 30 μm. (c) Immunohistochemistry of human αSyn in the SN after V1SSV2 injection. Tissue sections were counterstained with hematoxylin (blue). Scale bars: 100 μm (left), 10 μm (right). (d) immunofluorescent double staining for TH and human αSyn and their colocalization with venusYFP in the SN after V1SSV2 injection. (e) VenusYFP before and after proteinase K treatment (PK− and PK+) in the SN following V1SSV2 injection. Scale bar: 30 μm.

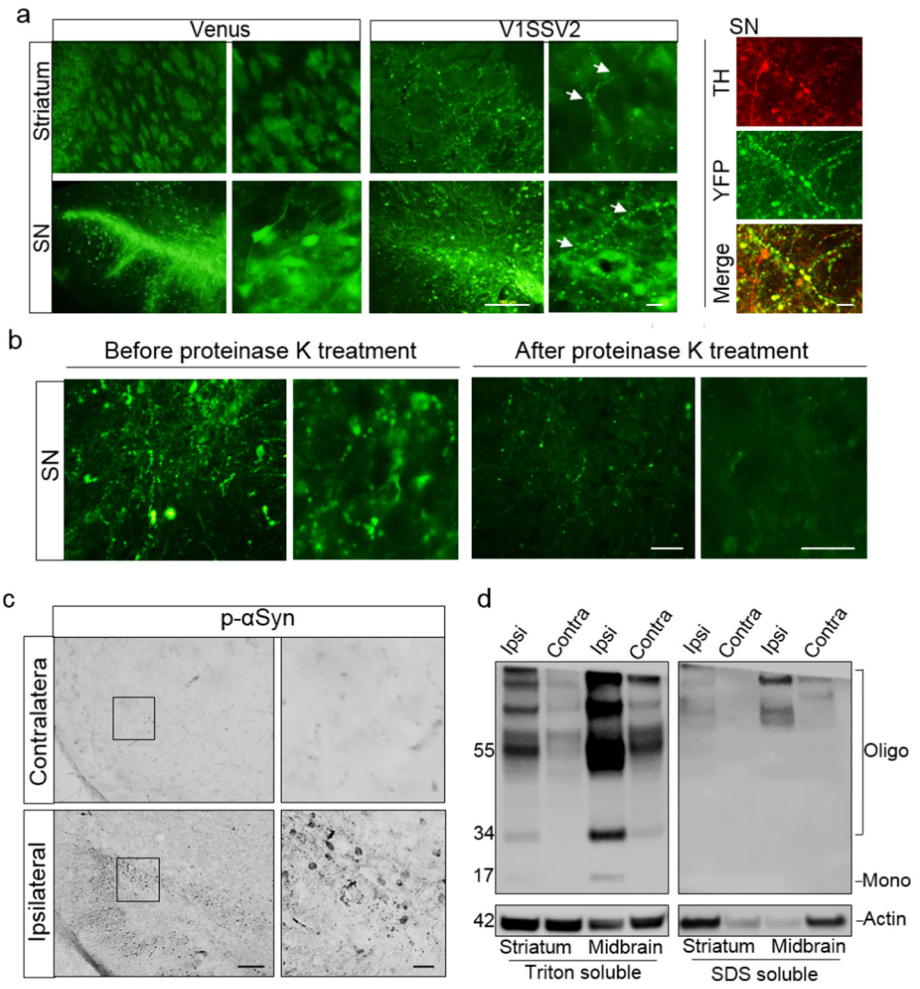

Fig. 2. Human αSyn transduction induces synucleinopathies. (a) VenusYFP fluorescence in the striatum, venusYFP fluorescence and its colacalization with TH in the SN 8 weeks following venus or V1SSV2 injection. Arrows indicate beaded, dystrophic neurites. Scale bars: 100 μm (left), 10 μm (right). (b) VenusYFP before and after proteinase K treatment in the SN 12 weeks following V1SSV2 injection. Scale bars: 20 μm. (c) Immunohistochemistry for pSer129 αSyn in the SN 12 weeks following V1SSV2 injection. Scale bars: 50 μm (left), 10 μm (right). (d) Accumulation of high-molecular-weight-αSyn species in the ventral midbrain and the striatum 8 weeks following V1SSV2 injection by Western blot analysis using anti-human αSyn antibody. Tissue sequential extractions were prepared using Triton X-100 and SDS.

αSyn have advanced preclinical therapeutic development as well as our understanding of PD pathophysiology. Based on the previous validation of AAV-mediated intranigral overexpression of human WT αSyn in rats and mice and the recent further development of an AAV8 human WT αSyn BiFC rat model, we report here successful application of this BiFC system in mice despite greater technical demands. The mouse model displays robust αSyn transduction and oligomerization, neuroinflammation, motor deficits, and reduced striatal DA and loss of dopaminergic neurons that are comparable to non-BiFC vectors.

Consistent with the rat model, overexpression and oligomerization of αSyn are detected by reconstituted venusYFP fluorescence, and further confirmed by our immunohistochemistry and immunoblotting using antibody against human αSyn. Intracellularly, venusYFP fluorescence is distributed in both cell bodies and neurites. In contrast to the demonstration of healthy cells transduced with venus, venusYFP fluorescence generated by αSyn oligomerization shows the appearance of distorted, punctate cellular morphology with beaded, dystrophic neurites, supporting pathogenic effects of αSyn oligomerization. Detection of venusYFP fluorescence and similar appearance of abnormal, beaded axon terminals in the striatum indicates effective anterograde transport of αSyn formed through the BiFC system along the nigrostriatal dopaminergic projections. Soluble oligomers are likely the pathological species in our model, which is overall consistent with our previous finding in rats (Dimant et al., 2013) though insoluble αSyn aggregates cannot be excluded given sparse but visible venusYFP fluorescence after proteinase K treatment at 12 weeks. Theoretically αSyn fibrils, if any, may also emit fluorescence. Using similar protein fragment complementation assay, we have detected in vitro the presence of extracellular αSyn oligomers and their detrimental effects on neighboring cells (Danzer and Kranich, 2012; Danzer et al., 2011). Our BiFC mouse model may facilitate detection of possible αSyn transmission in vivo.

Reduced striatal DA content, the core neurochemical feature of human PD, is demonstrated in our mouse models expressing human WT αSyn mediated by both BiFC and non-BiFC. With matching intensity of venusYFP fluorescence to venus control, BiFC αSyn induced a progressive reduction in DA levels in the striatum between 4 and 12 weeks after viral transduction. Reduced striatal DA has been reported in an AAV1/2 A53T αSyn mouse model with a similar virus titer at 10 weeks (Ip et al., 2017). This reduction appears to be dose-dependent as well, as demonstrated by non-BiFC αSyn overexpression, which induces corresponding 50% and 24% reduction at a higher titer and at a lower, half titer. The higher titer matches non-toxic empty vector. These findings suggest that the effect on striatal DA is likely related to αSyn-specific toxicity. Of note, at the same titer, venusYFP generates over 2-fold more intense venusYFP fluorescence than V1SSV2. This is expected since reconstruction of one venusYFP molecule takes at least two αSyn molecules. More venusYFP may explain reduced DA by high

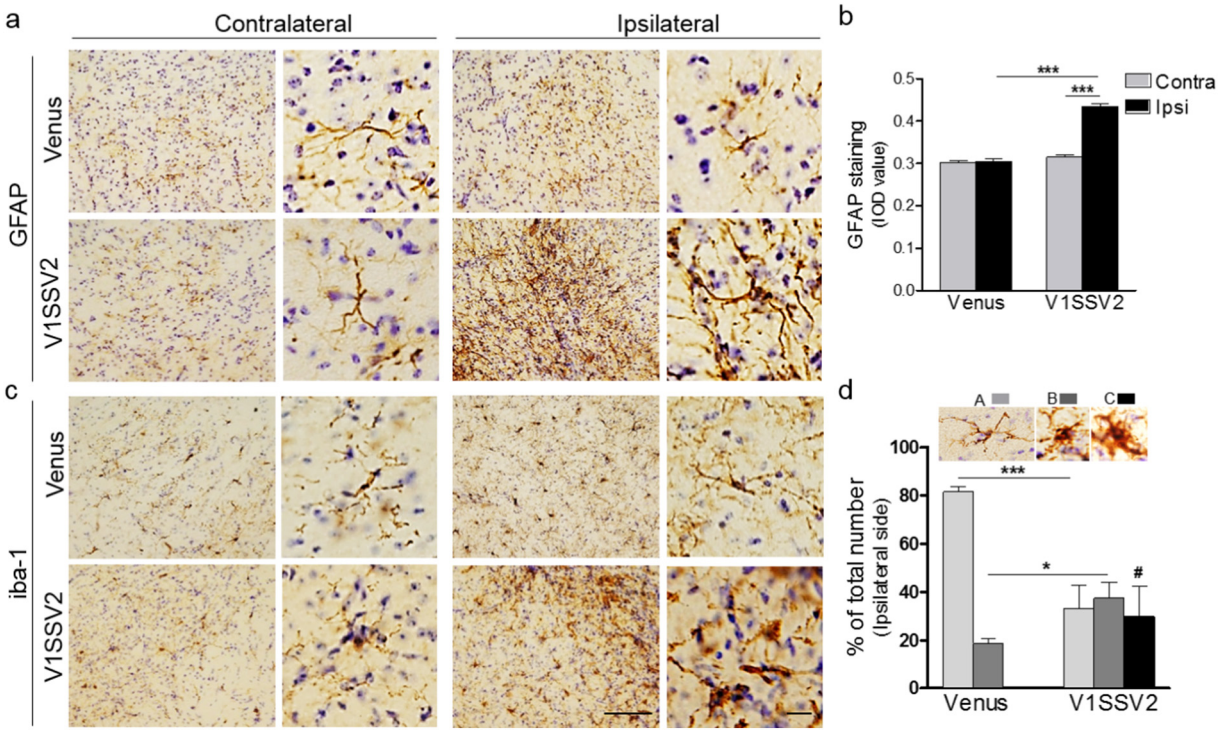

Fig. 3. Human αSyn overexpression in the SN triggers astrogliosis and microgliosis at 12 weeks post-AAV injection. (a) Midbrain coronal sections immunostained for GFAP from mice injected with venus or V1SSV2 injection. (b) Quantification of GFAP staining IOD. Venus, $n = 6$; V1SSV2, $n = 7$. (c) Midbrain coronal sections immunostained for iba1 from mice injected with venus or V1SSV2 injection. (d) Morphological classification of iba1-positive cells in the SNpc. Type A, resting, Type B, activated, Type C, phagocytic. $n = 4$ per group. Scale bars: 50 μm (left), 10 μm (right). Data are expressed as mean ± SEM $*p < 0.05$, $***p < 0.001$ ANOVA followed by Tukey's post hoc test. # indicates phagocytic microglia identified in V1SSV2 group only.

venus titer, which is not shown in mice injected with non-BiFC empty vector even at a higher titer, supporting toxicity of excessive venusYFP, not AAV8 itself (Klein et al., 2006).

Altered motor behavior is observed in our AAV αSyn mice. Increased travel distance, movement duration and velocity in open field are demonstrated. Although behavioral phenotypes in αSyn models are not

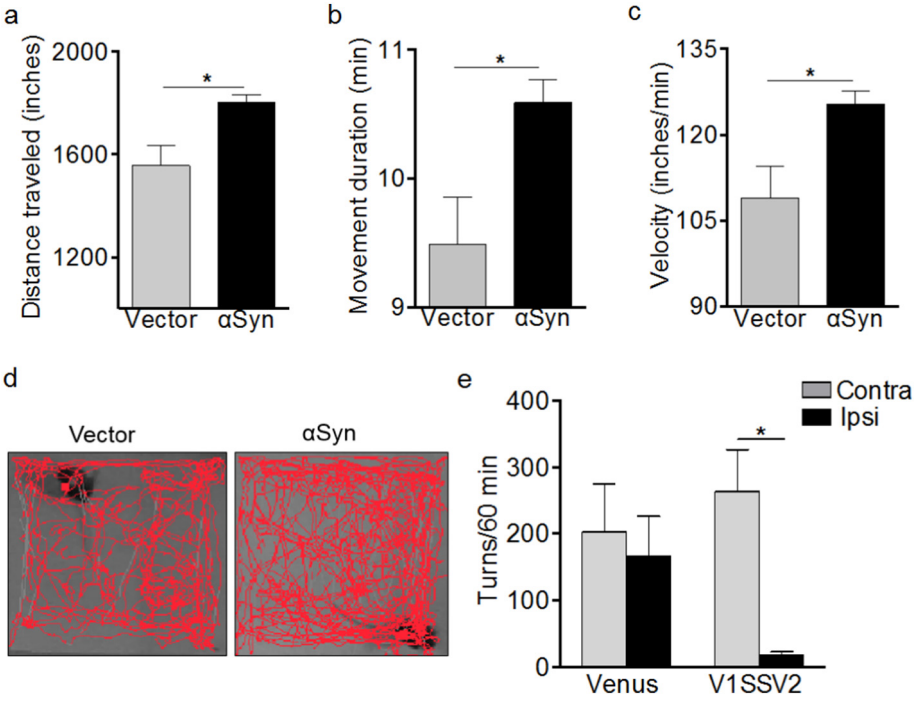

Fig. 4. Human αSyn expression in the SN is associated with abnormal locomotor activity and rotation behavior in mice. Total distance traveled (a), moving duration time (b), velocity (c) and representative movement tracks (d) by open field test 14 weeks post virus injection. $n = 5$ per group, average of data from two sessions. Amphetamine induced rotations 11 weeks post-injection (e). Venus, n = 6; V1SSV2, n = 7. Data are expressed as the means ± SEM $*p < 0.05$ student t-test (a–c), ANOVA followed by Turkey's post hoc test (e).

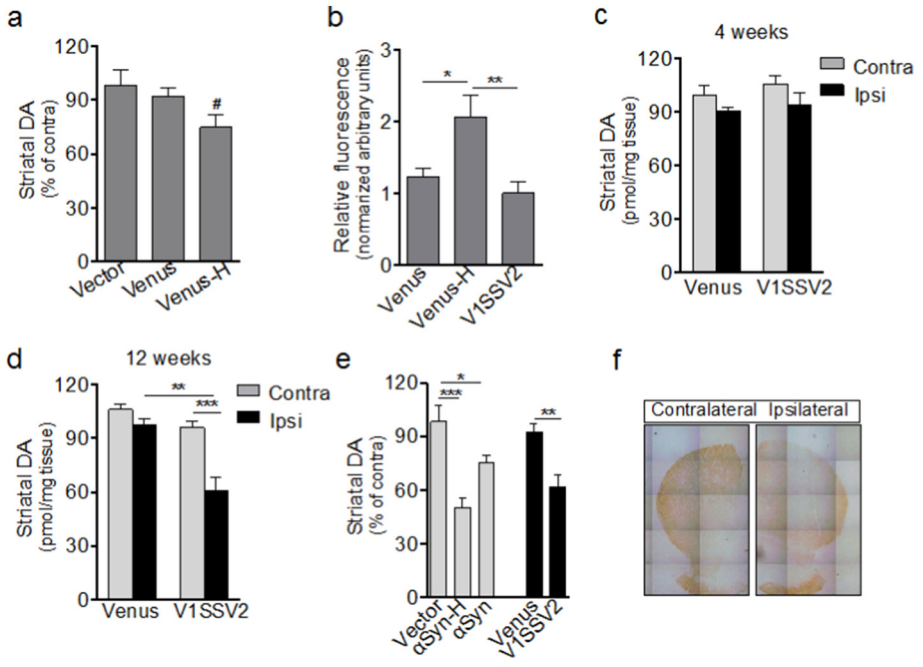

Fig. 5. Human αSyn expression in the SN leads to reduced striatal DA measured by HPLC. (a) Striatal DA levels. Vector, n = 4, Venus, n = 6, Venus-H, n = 7, 12 weeks post-injection. (b) YFP fluorescence intensity in the SN 4 weeks post-injection. V1SSV2, n = 7, Venus-H, Venus, *n* = 6. (c–d) Striatal DA levels 4 and 12 weeks post-injection. Venus/4 weeks, n = 7; V1SSV2/4 weeks, *n* = 8; Venus/12 weeks, n = 6, V1SSV2/12 weeks, *n* = 12. (e) Striatal DA levels from mice 12 weeks after injection with BiFC vectors (Venus and V1SSV2) and non-BiFC vectors (Vector, αSyn). Venus n = 6, V1SSV2, n = 12; vector, n = 4, αSyn-H, n = 12, αSyn, n = 7. (f) Representative striatal TH immunohistochemistry from a V1SSV2-injected mouse at 12 weeks. Data are expressed as the means ± SEM. #$p < 0.05$ student *t*-test, ipsilateral side vs contralateral side. $*p < 0.05$, $**p < 0.01$, $***p < 0.001$ ANOVA followed by Tukey's post hoc test.

well-established and often variable, motor deficits such as decreased locomotion are observed in αSyn transgenic mice (Graham and Sidhu, 2010; Koprich et al., 2017; Unger et al., 2006). Unexpected hyperactivity has been demonstrated in both A53T αSyn transgenic mice (Rothman et al., 2013), which can be attributed to anxiety (Farrell et al., 2014), and A30P αSyn transgenic mice (Freichel et al., 2007). However, hypo- or hyper- activities in these models do not always correlate with nigrostrital dopaminergic dysfunction (Chesselet and Richter, 2011; Koprich et al., 2017). Neither A53T nor A30P αSyn transgenic mice demonstrate significant dopaminergic cell death. It is possible that the motor abnormalities reflect neuronal dysfunction rather than dopaminergic neurodegeneration (Peelaerts and Bousset, 2015). A30P αSyn transgenic mice, for example, display increased extracellular DA at 6 months of age. The exact mechanisms underlying increased locomotor activity in our model are unclear. Similarly, it remains to be elucidated why BiFC αSyn mice tend to rotate contralateral to the lesion side. Typical parkinsonian behavioral changes such as motor hypoactivity and ipsilateral turns in unilateral models of PD are usually associated with extensive nigrostriatal lesion in the nigrostriatal pathway, mostly toxin induced (Schober, 2004). An AAV2/7 αSyn mouse model with ~70% nigral dopaminergic neuron death shows hypoactivities in open field (Oliveras-Salvá et al., 2013) and an AAV6 αSyn rat model with 80% loss of dopaminergic neurons display ipsilateral turns (Decressac et al., 2012). Compensatory modulation of DA receptors in response to relatively moderate DA reduction might also be involved in the unexpected behavioral changes in our model (Bezard and Gross, 1998; Stricker et al., 2011).

Our mouse models show time-dependent loss of dopaminergic neurons in the SN, the cardinal pathological feature of PD. Plateaued reduction by one third between 3 and 5 months following viral αSyn transduction is in agreement with previously reported mild (~25%) dopaminergic neuron loss in AAV αSyn mouse models (Cao et al., 2010; Harms et al., 2013; St Martin et al., 2007). Likewise, the lesion we demonstrated is slightly less than the average 45% dopaminergic neuron loss observed in rats (Dimant et al., 2013), as may be expected due to difference in species, virus titer (5 vs 8.5×10^{12} vg/ml) and time points (12 vs

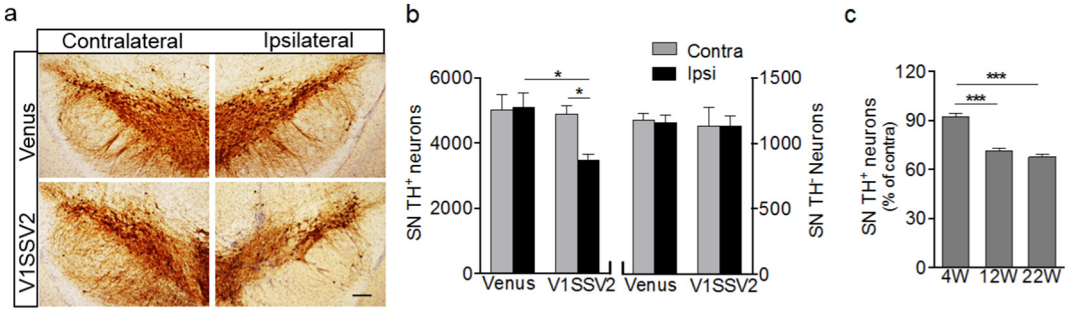

Fig. 6. Human αSyn expression in the SN leads to loss of dopaminergic neurons. (a) Representative SN sections immunostained for TH at 12 weeks post-injection. Scale bar: 100 μm. (b) Stereological quantification of nigral TH-positive and TH-negative cells 12 weeks post-injection. Venus, n = 4, V1SSV2, n = 6. (c) Stereological quantification of nigral TH-positive neurons from mice 4, 12, 22 weeks post- V1SSV2 injection. n = 6, n = 7, n = 4 per 4, 12, 22w groups. Data are expressed as the means ± SEM $*p < 0.05$, $***p < 0.001$, ANOVA followed by Tukey's post hoc test.

8 weeks). Demonstration of dopaminergic neuron loss at an earlier time point in BiFC αSyn mice at 12 weeks than typical 24 weeks in non-BiFC αSyn (Cao et al., 2010; Harms et al., 2013; St Martin et al., 2007) may be contributed to different virus serotype (AAV8 vs AAV2 or mixture of AAV2&8) (Albert et al., 2017; Klein et al., 2006; Watakabe et al., 2015). It has been demonstrated that aSyn multimerization in protein complementation assays is not driven by the tags (Outeiro et al., 2008; Wang et al., 2014), and we do not find evidence for enhanced effects of BiFC αSyn vs non-BiFC αSyn. The extent of nigral neuronal cell body loss is overall consistent with DA reduction (38%) in the striatum, suggesting αSyn-induced dopaminergic neurodegeneration in the SN as the main cause for associated DA depletion in the striatum.

The accompanying gliosis and microgliosis that we show in our BiFC αSyn mice are consistent with well-characterized neuroinflammation in AAV αSyn rat and mouse models, suggesting prolonged inflammatory responses and potential role of activated astrocytes and microglia in dopaminergic neurodegeneration triggered by αSyn. However, mechanisms contributing to eventual neurodegenerative consequences of human αSyn overexpression and oligomerization are not fully understood. Our systematically validated model facilitating fluorescence detection of αSyn oligomerization along with non-BiFC αSyn mouse model may provide a useful tool to investigate such underlying mechanisms and to explore therapeutic approaches for PD. AAV1/2 have been described to mediate αSyn overexpression in oligodendrocytes (Bassil et al., 2017). However, since the ability of our vectors to transduce glial cells has not been characterized, using this technique to model other synucleinopathies such as multiple system atrophy would require further validation.

Funding Sources

This work is supported by The National Institute of Neurological Disorders and Stroke (1R21NS090246-01A1 to X. C.), National Natural Science Foundation of China (81471293 to X.C., 81603452 to W.C.), the Michael J. Fox Foundation (9908 to X. C.), the Maximilian E. & Marion O. Hoffman Foundation (to M.A.S.), and the Milstein Medical Asian American Partnership Foundation (2015 to fellow W. C. and mentor X. C.). The funding sources do not have any role in the writing of the manuscript or the decision to submit it for publication. The authors have not been paid to write this article by a pharmaceutical company or other agency.

Conflicts of Interest

None.

Author Contributions

W.C., M.A.S, P.J.M and X.C. contributed to conception and design of the study. W.C., D.F. and X.C. contributed to acquisition and analysis of data. W.C. and X.C. wrote the article.

References

Albert, K., Voutilainen, M., Domanskyi, A., Airavaara, M., 2017. AAV vector-mediated gene delivery to substantia Nigra dopamine neurons: implications for gene therapy and disease models. Genes 8:63. https://doi.org/10.3390/genes8020063.

Anderson, J.P., Walker, D.E., Goldstein, J.M., De Laat, R., Banducci, K., Caccavello, R.J., Barbour, R., Huang, J., Kling, K., Lee, M., Diep, L., Keim, P.S., Shen, X., Chataway, T., Schlossmacher, M.G., Seubert, P., Schenk, D., Sinha, S., Gai, W.P., Chilcote, T.J., 2006. Phosphorylation of Ser-129 is the dominant pathological modification of α-synuclein in familial and sporadic lewy body disease. J. Biol. Chem. 281: 29739–29752. https://doi.org/10.1074/jbc.M600933200.

Bassil, F., Guerin, P.A., Dutheil, N., Li, Q., Klugmann, M., Meissner, W.G., Bezard, E., Fernagut, P.O., 2017. Viral-mediated oligodendroglial alpha-synuclein expression models multiple system atrophy. Mov. Disord. 32:1230–1239. https://doi.org/10.1002/mds.27041.

Bengoa-Vergniory, N., Roberts, R.F., Wade-Martins, R., Alegre-Abarrategui, J., 2017. Alpha-synuclein oligomers: a new hope. Acta Neuropathol.:1–20 https://doi.org/10.1007/s00401-017-1755-1.

Bezard, E., Gross, C.E., 1998. Compensatory mechanisms in experimental and human parkinsonism: towards a dynamic approach. Prog. Neurobiol. https://doi.org/10.1016/S0301-0082(98)00006-9.

Braak, H., Del Tredici, K., 2009. Neuroanatomy and pathology of sporadic Parkinson's disease. Adv. Anat. Embryol. Cell Biol. https://doi.org/10.1007/978-3-540-79850-7_1.

Braak, H., Sastre, M., Del Tredici, K., 2007. Development of α-synuclein immunoreactive astrocytes in the forebrain parallels stages of intraneuronal pathology in sporadic Parkinson's disease. Acta Neuropathol. 114:231–241. https://doi.org/10.1007/s00401-007-0244-3.

Brooks, S.P., Dunnett, S.B., 2009. Tests to assess motor phenotype in mice: a user's guide. Nat. Rev. Neurosci. 10:519–529. https://doi.org/10.1038/nrn2652.

Cao, S., Theodore, S., Standaert, D.G., 2010. Fcγ receptors are required for NF-κB signaling, microglial activation and dopaminergic neurodegeneration in an AAV-synuclein mouse model of Parkinson's disease. Mol. Neurodegener. 5:42. https://doi.org/10.1186/1750-1326-5-42.

Chen, X., Burdett, T.C., Desjardins, C.A., Logan, R., Cipriani, S., Xu, Y., Schwarzschild, M.A., 2013. Disrupted and transgenic urate oxidase alter urate and dopaminergic neurodegeneration. Proc. Natl. Acad. Sci. 110:300–305. https://doi.org/10.1073/pnas.1217296110.

Chen, X., Chen, H., Cai, W., Maguire, M., Ya, B., Zuo, F., Logan, R., Li, H., Robinson, K., Vanderburg, C.R., Yu, Y., Wang, Y., Fisher, D.E., Schwarzschild, M.A., 2017. The melanoma-linked "redhead" MC1R influences dopaminergic neuron survival. Ann. Neurol. 81:395–406. https://doi.org/10.1002/ana.24852.

Chesselet, M.-F., Richter, F., 2011. Modelling of Parkinson's disease in mice. Lancet Neurol. 10:1108–1118. https://doi.org/10.1016/S1474-4422(11)70227-7.

Danzer, K., Kranich, L., 2012. Exosomal cell-to-cell transmission of alpha synuclein oligomers. Mol. Neurodegen. 7:42. https://doi.org/10.1186/1750-1326-7-42.

Danzer, K.M., Ruf, W.P., Putcha, P., Joyner, D., Hashimoto, T., Glabe, C., Hyman, B.T., McLean, P.J., 2011. Heat-shock protein 70 modulates toxic extracellular -synuclein oligomers and rescues trans-synaptic toxicity. FASEB J. 25:326–336. https://doi.org/10.1096/fj.10-164624.

Decressac, M., Mattsson, B., Lundblad, M., Weikop, P., Björklund, A., 2012. Progressive neurodegenerative and behavioural changes induced by AAV-mediated overexpression of α-synuclein in midbrain dopamine neurons. Neurobiol. Dis. 45:939–953. https://doi.org/10.1016/j.nbd.2011.12.013.

Dehay, B., Bourdenx, M., Gorry, P., Przedborski, S., Vila, M., Hunot, S., Singleton, A., Olanow, C.W., Merchant, K.M., Bezard, E., Petsko, G.A., Meissner, W.G., 2015. Targeting α-synuclein for treatment of Parkinson's disease: mechanistic and therapeutic considerations. Lancet Neurology. https://doi.org/10.1016/S1474-4422(15)00006-X.

Dimant, H., Kalia, S.K., Kalia, L.V., Zhu, L.N., Kibuuka, L., Ebrahimi-Fakhari, D., McFarland, N.R., Fan, Z., Hyman, B.T., McLean, P.J., 2013. Direct detection of alpha synuclein oligomers in vivo. Acta Neuropathol. Commun. 1:6. https://doi.org/10.1186/2051-5960-1-6.

Farrell, K.F., Krishnamachari, S., Villanueva, E., Lou, H., Alerte, T.N.M., Peet, E., Drolet, R.E., Perez, R.G., 2014. Non-motor parkinsonian pathology in aging A53T α-Synuclein mice is associated with progressive synucleinopathy and altered enzymatic function. J. Neurochem. 128:536–546. https://doi.org/10.1111/jnc.12481.

Freichel, C., Neumann, M., Ballard, T., Müller, V., Woolley, M., Ozmen, L., Borroni, E., Kretzschmar, H., Haass, C., Spooren, W., Kahle, P.J., 2007. Age-dependent cognitive decline and amygdala pathology in alpha-synuclein transgenic mice. Neurobiol. Aging 28:1421–1435. https://doi.org/10.1016/j.neurobiolaging.2006.06.013.

Graham, D.R., Sidhu, A., 2010. Mice expressing the A53T mutant form of human alpha-synuclein exhibit hyperactivity and reduced anxiety-like behavior. J. Neurosci. Res. 88:1777–1783. https://doi.org/10.1002/jnr.22331.

Harms, A.S., Cao, S., Rowse, A.L., Thome, A.D., Li, X., Mangieri, L.R., Cron, R.Q., Shacka, J.J., Raman, C., Standaert, D.G., 2013. MHCII is required for -synuclein-induced activation of microglia, CD4 T cell proliferation, and dopaminergic neurodegeneration. J. Neurosci. 33:9592–9600. https://doi.org/10.1523/JNEUROSCI.5610-12.2013.

Hirsch, E.C., Hunot, S., 2009. Neuroinflammation in Parkinson's disease: a target for neuroprotection? Lancet Neurology. https://doi.org/10.1016/S1474-4422(09)70062-6.

Hirsch, E.C., Vyas, S., 2012. Parkinsonism and related disorders neuroinflammation in Parkinson's disease. Parkinsonism Relat. Disord. 18S1:S210–S212. https://doi.org/10.1016/S1353-8020(11)70065-7.

Hirsch, E.C., Hunot, S., Hartmann, A., 2005. Neuroinflammatory processes in Parkinson's disease. Parkinsonism and Related Disorders https://doi.org/10.1016/j.parkreldis.2004.10.013.

Iancu, R., Mohapel, P., Brundin, P., Paul, G., 2005. Behavioral characterization of a unilateral 6-OHDA-lesion model of Parkinson's disease in mice. Behav. Brain Res. 162:1–10. https://doi.org/10.1016/j.bbr.2005.02.023.

Ip, C.W., Klaus, L.-C., Karikari, A.A., Visanji, N.P., Brotchie, J.M., Lang, A.E., Volkmann, J., Koprich, J.B., 2017. AAV1/2-induced overexpression of A53T-α-synuclein in the substantia nigra results in degeneration of the nigrostriatal system with Lewy-like pathology and motor impairment: a new mouse model for Parkinson's disease. Acta Neuropathol. Commun. 5, 11. https://doi.org/10.1186/s40478-017-0416-x.

Kalia, L.V., Kalia, S.K., McLean, P.J., Lozano, A.M., Lang, A.E., 2013. α-Synuclein oligomers and clinical implications for parkinson disease. Ann. Neurol. 73:155–169. https://doi.org/10.1002/ana.23746.

Kalinderi, K., Bostantjopoulou, S., Fidani, L., 2016. The genetic background of Parkinson's disease: current progress and future prospects. Acta Neurol. Scand. 134:314–326. https://doi.org/10.1111/ane.12563.

Kingwell, K., 2017. Zeroing in on Neurodegenerative α-synuclein. https://doi.org/10.1038/nrd.2017.95.

Klein, R.L., Dayton, R.D., Leidenheimer, N.J., Jansen, K., Golde, T.E., Zweig, R.M., 2006. Efficient neuronal gene transfer with AAV8 leads to neurotoxic levels of tau or green fluorescent proteins. Mol. Ther. 13:517–527. https://doi.org/10.1016/j.ymthe.2005.10.008.

Koprich, J.B., Kalia, L.V., Brotchie, J.M., 2017. Animal models of α-synucleinopathy for Parkinson disease drug development. Nat. Rev. Neurosci. https://doi.org/10.1038/nrn.2017.75.

McFarland, N.R., Fan, Z., Xu, K., Schwarzschild, M.A., Feany, M.B., Hyman, B.T., McLean, P.J., 2009. Alpha-synuclein S129 phosphorylation mutants do not alter nigrostriatal toxicity in a rat model of Parkinson disease. J. Neuropathol. Exp. Neurol. 68:515–524. https://doi.org/10.1097/NEN.0b013e3181a24b53.

More, S.V., Kumar, H., Kim, I.S., Song, S.Y., Choi, D.K., 2013. Cellular and molecular mediators of neuroinflammation in the pathogenesis of Parkinson's disease. Mediat. Inflamm. https://doi.org/10.1155/2013/952375.

Oliveras-Salvá, M., Van der Perren, A., Casadei, N., Stroobants, S., Nuber, S., D'Hooge, R., Van den Haute, C., Baekelandt, V., 2013. rAAV2/7 vector-mediated overexpression of alpha-synuclein in mouse substantia nigra induces protein aggregation and progressive dose-dependent neurodegeneration. Mol. Neurodegener. 8:44. https://doi.org/10.1186/1750-1326-8-44.

Outeiro, T.F., Putcha, P., Tetzlaff, J.E., Spoelgen, R., Koker, M., Carvalho, F., Hyman, B.T., McLean, P.J., 2008. Formation of toxic oligomeric α-synuclein species in living cells. PLoS One 3. https://doi.org/10.1371/journal.pone.0001867.

Paulmurugan, R., Massoud, T.F., Huang, J., Gambhir, S.S., 2004. Molecular imaging of drug-modulated protein-protein interactions in living subjects. Cancer Res. 64:2113–2119. https://doi.org/10.1158/0008-5472.CAN-03-2972.

Peelaerts, W., Bousset, L., 2015. Synuclein strains cause distinct synucleinopathies after local and systemic administration. Nature 522 (7556):340–344. https://doi.org/10.1038/nature14547.

Perry, V.H., Holmes, C., 2014. Microglial priming in neurodegenerative disease. Nat. Rev. Neurol. 10:217–224. https://doi.org/10.1038/nrneurol.2014.38.

Rothman, S.M., Griffioen, K.J., Vranis, N., Ladenheim, B., Cong, W.N., Cadet, J.L., Haran, J., Martin, B., Mattson, M.P., 2013. Neuronal expression of familial Parkinson's disease A53T α-synuclein causes early motor impairment, reduced anxiety and potential sleep disturbances in mice. J. Parkinson's Dis. 3:215–229. https://doi.org/10.3233/JPD-120130.

Sanchez-Guajardo, V., Febbraro, F., Kirik, D., Romero-Ramos, M., 2010. Microglia acquire distinct activation profiles depending on the degree of α-synuclein neuropathology in a rAAV based model of Parkinson's disease. PLoS One 5. https://doi.org/10.1371/journal.pone.0008784.

Schober, A., 2004. Classic toxin-induced animal models of Parkinson's disease: 6-OHDA and MPTP. Cell Tissue Res. https://doi.org/10.1007/s00441-004-0938-y.

Spillantini, M.G., Schmidt, M.L., Lee, V.M.-Y., Trojanowski, J.Q., Jakes, R., Goedert, M., 1997. alpha-Synuclein in Lewy bodies. Nature 388:839–840. https://doi.org/10.1038/42166.

St Martin, J.L., Klucken, J., Outeiro, T.F., Nguyen, P., Keller-McGandy, C., Cantuti-Castelvetri, I., Grammatopoulos, T.N., Standaert, D.G., Hyman, B.T., McLean, P.J., 2007. Dopaminergic neuron loss and up-regulation of chaperone protein mRNA induced by targeted over-expression of alpha-synuclein in mouse substantia nigra. J. Neurochem. 100:1449–1457. https://doi.org/10.1111/j.1471-4159.2006.04310.x.

Stricker, E.M., Zigmond, M.J., Stricker, E.M., Zigmond, M.J., 2011. Brain Monoamines, Homeostasis, and Adaptive Behavior, in: Comprehensive Physiology. John Wiley & Sons, Inc., Hoboken, NJ, USA https://doi.org/10.1002/cphy.cp010413.

Tetzlaff, J.E., Putcha, P., Outeiro, T.F., Ivanov, A., Berezovska, O., Hyman, B.T., McLean, P.J., 2008. CHIP targets toxic α-synuclein oligomers for degradation. J. Biol. Chem. 283:17962–17968. https://doi.org/10.1074/jbc.M802283200.

Theodore, S., Cao, S., McLean, P.J., Standaert, D.G., 2008. Targeted overexpression of human alpha-synuclein triggers microglial activation and an adaptive immune response in a mouse model of Parkinson disease. J. Neuropathol. Exp. Neurol. 67:1149–1158. https://doi.org/10.1097/NEN.0b013e31818e5e99.Targeted.

Unger, E.L., Eve, D.J., Perez, X.A., Reichenbach, D.K., Xu, Y., Lee, M.K., Andrews, A.M., 2006. Locomotor hyperactivity and alterations in dopamine neurotransmission are associated with overexpression of A53T mutant human α-synuclein in mice. Neurobiol. Dis. 21:431–443. https://doi.org/10.1016/j.nbd.2005.08.005.

Wang, L., Das, U., Scott, D.A., Tang, Y., McLean, P.J., Roy, S., 2014. α-Synuclein multimers cluster synaptic vesicles and attenuate recycling. Curr. Biol. 24:2319–2326. https://doi.org/10.1016/j.cub.2014.08.027.

Watakabe, A., Ohtsuka, M., Kinoshita, M., Takaji, M., Isa, K., Mizukami, H., Ozawa, K., Isa, T., Yamamori, T., 2015. Comparative analyses of adeno-associated viral vector serotypes 1, 2, 5, 8 and 9 in marmoset, mouse and macaque cerebral cortex. Neurosci. Res. 93:144–157. https://doi.org/10.1016/j.neures.2014.09.002.

West, M.J., Slomianka, L., Gundersen, H.J.G., 1991. Unbiased stereological estimation of the total number of neurons in the subdivisions of the rat hippocampus using the optical fractionator. Anat. Rec. 231:482–497. https://doi.org/10.1002/ar.1092310411.

Xiao, D., Bastia, E., Xu, Y.-H., Benn, C.L., Cha, J.-H.J., Peterson, T.S., Chen, J.-F., Schwarzschild, M.A., 2006. Forebrain adenosine A2A receptors contribute to L-3,4-dihydroxyphenylalanine-induced dyskinesia in hemiparkinsonian mice. J. Neurosci. 26:13548–13555. https://doi.org/10.1523/JNEUROSCI.3554-06.2006.